Comparison of the adsorption of Zn(II) on α- and γ-MnO_2 nanostructures

Van Phuc Dinh[1*], Ngoc Chung Le[2], Ngoc Tuan Nguyen[3], Thien Hoang Ho[1], Van Dong Nguyen[4]

[1]*Dong Nai University*
[2]*Dalat University*
[3]*Vietnam Atomic Energy Institute*
[4]*University of Science, Vietnam National University, Ho Chi Minh city*

Received 11 April 2017; accepted 28 August 2017

Abstract:

In this report, the adsorption of Zn(II) ion on γ- and α-MnO_2 nanostructures was compared. The results showed that the maximum adsorption was obtained at pH = 4.0 for both materials and after 60 minutes for γ-MnO_2 and 80 minutes for α-MnO_2. Adsorption isotherm models demonstrated that the Langmuir was the best model to describe the adsorption of Zinc(II) on γ- and α-MnO_2 because of the highest correlation coefficient (R^2), the smallest root mean square error (RMSE), and the nonlinear chi-squared test (χ^2) values. The maximum adsorption capacity of γ-MnO_2 calculated from Langmuir model was 55.23 mg/g, which was roughly double α-MnO_2. The lower 1/n value from Freundlich model for α-MnO_2 revealed that it was not as favourable as γ-MnO_2. The heat of the adsorption as well as the mean free energy estimated from Temkin and Dubinin - Radushkevich models to be less than 8 kJ/mol indicated that the adsorption on both materials followed a physical process. Kinetic studies showed that pseudo-second-order model was accurate to describe both materials in three stages.

Keywords: *adsorption, kinetics, Zinc, α-MnO_2, γ-MnO_2.*

Classification number: *2.2*

Introduction

Zinc is an essential trace element that can be found in cells throughout the human body as well as animals and plants. However, Zinc can cause depression, lethargy, neurological signs, and excessive thirst [1]. Zinc is widely used in many important industrial applications such as mining, coal and waste combustion, and steel processing [2]. Various treatment techniques have been applied to remove Zinc(II) ions from contaminated water such as chemical precipitation, flotation, adsorption, ion exchange, and electrochemical deposition [3]. Adsorption technology is considered as one of the most efficient and promising methods for the treatment of trace amount of heavy metal ions in a large volume of water because of its enrichment efficiency and the ease of phase separation [4-9].

Manganese dioxide is a low-cost and environmentally friendly material. Along with many types of crystalline structures such as α-, β-, and γ-, etc., manganese dioxide has been extensively studied due to its excellent chemical characteristics. Therefore, this material is applied in different areas such as batteries, molecular sieves, catalysts, and adsorbents [10-12]. However, a systematic comparison of the adsorption of Zn(II) from the aqueous solution onto α- and γ-MnO_2 nanomaterials has not been reported.

Our goal is to compare the adsorption capacity of Zinc(II) from aqueous solution by using α- and γ-MnO_2 nanomaterials as adsorbents. Four non-linear adsorption isotherm models, namely Langmuir, Freundlich, Temkin, and Dubinin - Radushkevich and three kinetic models, namely pseudo-first-order, pseudo-second-order, and intra-diffusion were used to assess the uptake capacity and to predict the adsorption mechanism.

Material and methods

Chemicals

Potassium permanganate ($KMnO_4$), ethyl alcohol (C_2H_5OH), HNO_3, and NaOH with analytical grade were purchased from Merck. Zn(II) ion was used as the adsorbate. 1000 mg/l of zinc standard stock solution was prepared by dissolving $Zn(NO_3)_2$ respectively in double-distilled water.

Analytical methods

Atomic Absorption Spectrometry (flame technique) was used to determine the concentration of zinc in aqueous solution by using an atomic absorption spectrophotometer AA - 7000 (Shimadzu, Japan).

The pH measurements were done with a pH-meter (MARTINI Instruments Mi-150 Romania) which was standardized by using HANNA instruments with three buffer solutions with the pH values of 4.01±0.01, 7.01±0.01, and 10.01±0.01.

Temperature-controlled shaker (Model IKA R5) was used for the equilibrium studies.

[*]*Corresponding author: Email: dinhvanphuc82@gmail.com*

Preparation α-MnO_2 and γ-MnO_2

The γ-MnO_2 was successfully synthesized by L. Ngoc Chung and D. Van Phuc [11] from ethanol and potassium permanganate; whereas, α-MnO_2 was formed by heating γ-MnO_2 at 600^{0}C [12]. The synthesized γ-MnO_2 and α-MnO_2 characterized by X-ray Diffractometer D5000 with X-ray radiation: CuKα, λ = 1.54056Å, Ultra High Resolution Scanning Electron Microscopy S - 4800, Transmission Electron Microscope with physical absorption system Micrometrics Gemini VII, and BET-BJH analysis were used as absorbents to adsorb Zinc(II) ions from aqueous solution.

Adsorption study

0.1 g of adsorbents was placed into 50 ml of Zn(II) ion solution in a 100 ml conical flask. The effect of pH (2-6), contact time (20-240 min), and initial concentration of Zn(II) ions were examined. The obtained mixture was centrifuged at 5500 rpm within 10 minutes, then was purified by PTFE Syring Filters with 0.22 µm of pore size to get the filtrate. The concentrations of Zn(II) ions in the filtrate before and after the adsorption were determined by F- ASS.

The adsorption capacity was calculated by using the mass balance equation for the adsorbent [12].

$$q = \frac{(C_o - C_e).V}{m} \quad (1)$$

The removal efficiency (%) was calculated using the following formula:

$$\%\ \text{Removal} = \frac{(C_o - C_e).100\%}{C_o} \quad (2)$$

where: q is the adsorption capacity (mg/g) at equilibrium, C_o and C_e are the initial and the equilibrium concentrations (mg/l), respectively. V is the volume (l) of the solution, and m is the mass (g) of the adsorbent used.

Some adsorption isotherm formula and kinetic models which were applied to predict both the adsorption capacities of materials and the adsorption mechanisms were given in Table 1 and Table 2 [13].

Table 1. The non-linear, error functions, and meaning of some models.

Isotherm	Non-linear form	Meaning	List of error functions
Langmuir	$q_e = \frac{q_m.K_L.C_e}{1+K_L.C_e}$	Assuming the adsorption occurred on monolayer on the material surface. Also, estimating the maximum adsorption capacity on the material surface.	$R^2 = 1 - \frac{\sum_{n=1}^{n}\left(q_{e,meas} - q_{e,calc}\right)^2}{\sum_{n=1}^{n}\left(q_{e,meas} - \overline{q_{e,calc}}\right)^2}$
Freundlich	$q_e = K_F.C_e^{1/n}$	Assuming the adsorption occurred on multilayers on the material surface.	$RMSE = \sqrt{\frac{1}{n-1}\sum_{n=1}^{n}\left(q_{e,meas} - q_{e,calc}\right)^2}$
Temkin	$q_e = \frac{RT}{b_T} Ln(K_T C_e)$	Evaluating the adsorption potentials of the adsorbent for adsorbates as well as the heat of the adsorption process.	$\chi^2 = \sum_{n=1}^{n}\frac{\left(q_{e,meas} - q_{e,calc}\right)^2}{q_{e,calc}}$
Dubinin - Radushkevich	$q_e = q_m.e^{(-\beta.\varepsilon^2)}$	Evaluating the value of mean sorption energy which gives information about chemical and physical sorption	The small values of RMSE and χ^2 indicate firstly a better fitting model, and secondly the correspondence of the model with the experimental data.

Where: q_e: the adsorption capacity at equilibrium (mg/g); q_m: the maximum adsorption capacity (mg/g); C_e: the equilibrium concentration (mg/l); K_L: Langmuir constant; K_F: Freundlich constant; n: adsorption intensity; R: the universal gas constant (8.314.10^{-3} kJ/K.mol); T: the temperature (K); b_T: Temkin isotherm constant related to the adsorption heat (kJ/mol); K_T: the equilibrium binding constant (l/mol); β: Dubinin-Radushkevich isotherm constant (mol^2/kJ^2); ε: Dubinin-Radushkevich isotherm constant; E: mean free energy (kJ/mol); R^2: correlation coefficient; RMSE: Root mean square error; χ^2: Non-linear chi-squared test.

Table 2. Models and kinetic parameters.

Kinetic models		Kinetic parameters		
			γ- MnO_2	α- MnO_2
		$q_{e\,(exp)}$ (mg/g)	25.5 mg/g	
Pseudo-first-order model	$\log(q_e - q_t) = \log q_e - \frac{k_1.t}{2,303}$	K_1(min)	7.60.10^{-3}	0.0166
		R^2	0.5594	0.7323
		$q_{e\,(cal)}$ (mg/g)	1.88	7.00
Pseudo-second-order model	$\frac{t}{q} = \frac{1}{k_2 q_e^2} + \left(\frac{1}{q_e}\right).t$	K_2 (g/mg.min)	0.06	5.86.10^{-3}
		R^2	1.0000	0.9982
		$q_{e\,(cal)}$ (mg/g)	24.94	25.91
Intra-particle diffusion model	$q_t = k_d t^{1/2} + C$	k_1	4.209	1.741
		k_2	0.3078	0.1164
		k_3	0.0026	-0.0025

Where: q_e: the amount of solute adsorbed at equilibrium per unit weight of adsorbent (mg/g); q: the amount of solute adsorbed at any time (mg/g); k_1, k_2, k_d: the adsorption constant; t, $t^{1/2}$: adsorption time.

Results and discussions

Characterization of γ- and α-MnO_2 nanomaterials

Figure 1 shows the X-ray diffraction patterns of two samples at room temperature and at 600^{0}C. The results indicated that γ-MnO_2 was formed at room temperature with some specific peaks at 2θ = 22.2^0, 37.8^0, 42.5^0, 56.3^0, and 65.7^0 corresponded with orthorhombic γ-MnO_2 (JCPDS card No. 82-2169); whereas, α-MnO_2 was formed by heating γ-MnO_2 at 600^{0}C with specific peaks at 2θ = 28.58^0, 37.48^0, 49.78^0, 59.98^0, and 68.98^0 (JCPDS card No. 01-072-1982). Surface properties, which affect the adsorption capacity of both materials, were determined by Scanning Electron Microscope (SEM) (Fig. 2) and TEM (Fig. 3). The comparison between SEM and TEM images of γ-MnO_2 and α-MnO_2 provided that γ-MnO_2 nanomaterial had a porous surface including many nanospheres while α-MnO_2 consisted of a lot of nanorods which were bigger than nanospheres. Moreover, the surface area of γ-MnO_2 was 65.00 m^2/g, which was approximately 6.5 times higher than that of α-MnO_2 (about 9.37 m^2/g) (Table 3). It can be predicted that adsorption properties of γ-MnO_2 were more favourable than that of α-MnO_2.

Investigation of factors affecting the adsorption

The pH and adsorption contact time are important factors affecting the adsorption of Zinc(II) ions on α- and γ-MnO_2 nanomaterials. As shown in Fig. 4A, at low pH values, the uptake of Zn(II) onto these materials was lower because the H^+ ions effectively compete with the Zn^{2+} [14]. At high pH values, the adsorption of Zinc(II) ion also decreased due to the formation of different types of Zinc(II) such as $Zn(OH)^+$, $Zn(OH)_2$ or ZnO_2^{2-} [15]. Although the charging behaviour of MnO_2 could induce

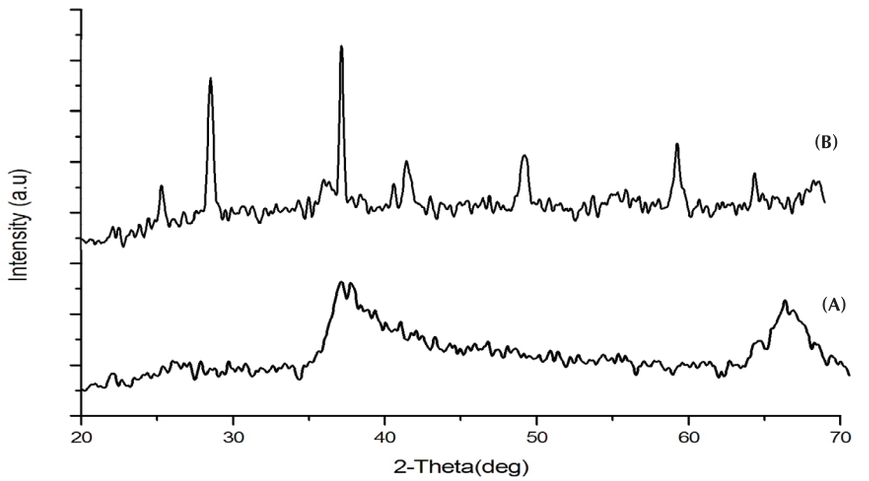

Fig. 1. XRD patterns of γ-MnO_2 (A) and α-MnO_2 (B).

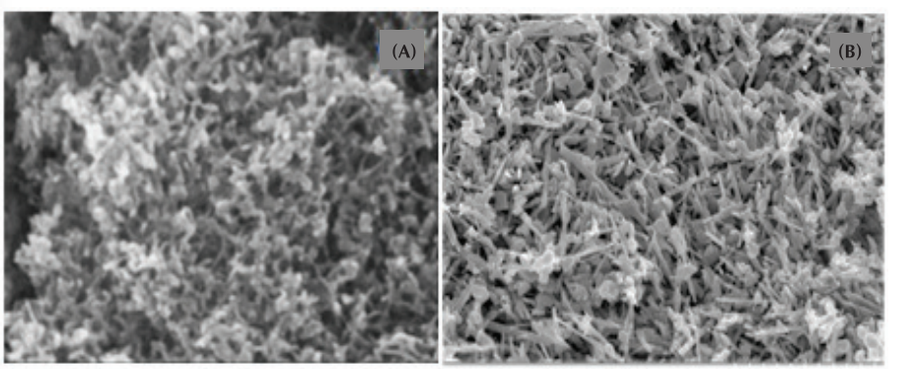

Fig. 2. SEM images of γ-MnO_2 (A) and α-MnO_2 (B).

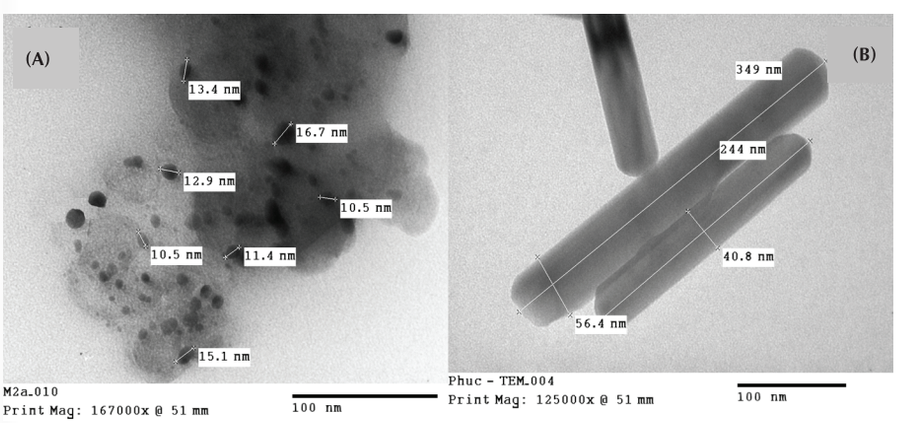

Fig. 3. TEM images of γ-MnO_2 (A) and α-MnO_2 (B).

Table 3. BET and BJH analysis results of γ-MnO_2 and α-MnO_2.

Materials	BET surface area	BJH adsorption pore size	BJH desorption pore size
γ-MnO_2	65.00 m^2/g	417.83 Å	340.23 Å
α-MnO_2	9.37 m^2/g	162.95A^0	734.37A^0

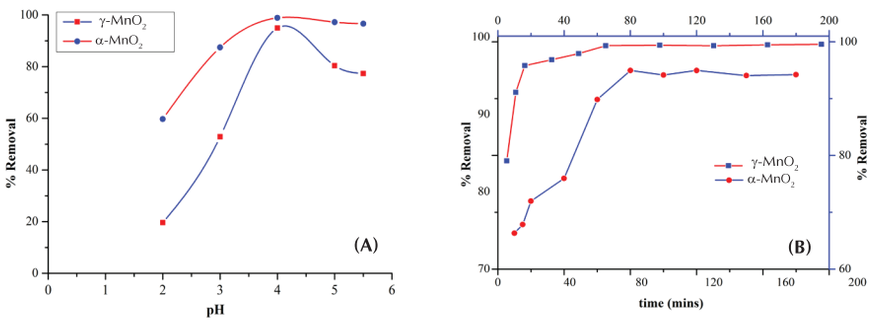

Fig. 4. The influence of pH (A) and adsorption contact time (B) to the removal of Zinc(II) by α- and γ-MnO_2 (240 rpm of shaking speed and 50 ppm of initial concentration).

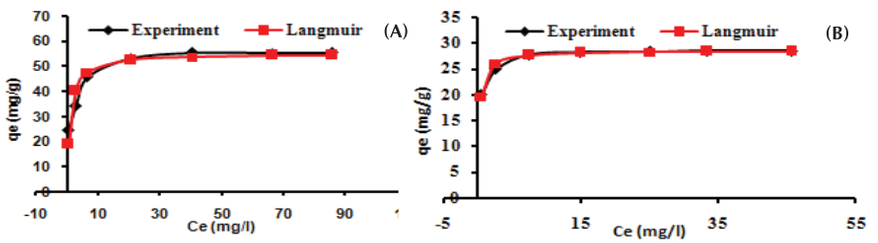

Fig. 5. Plots of non-linear isotherm Langmuir models of γ-MnO_2 (A) and α-MnO_2 (B).

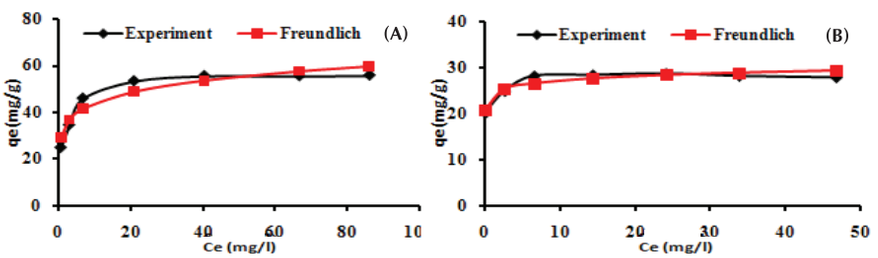

Fig. 6. Plots of non-linear isotherm Freundlich models of γ-MnO_2 (A) and α-MnO_2 (B).

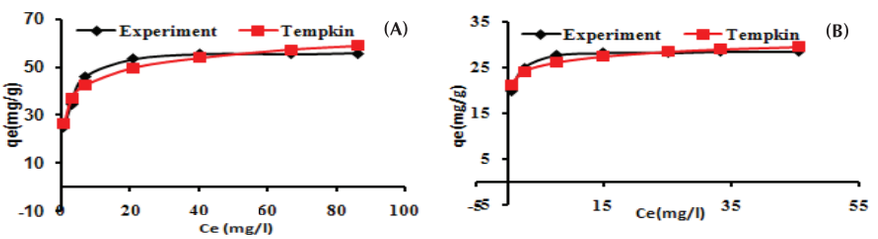

Fig. 7. Plots of non-linear isotherm Temkin models of γ-MnO_2 (A) and α-MnO_2 (B).

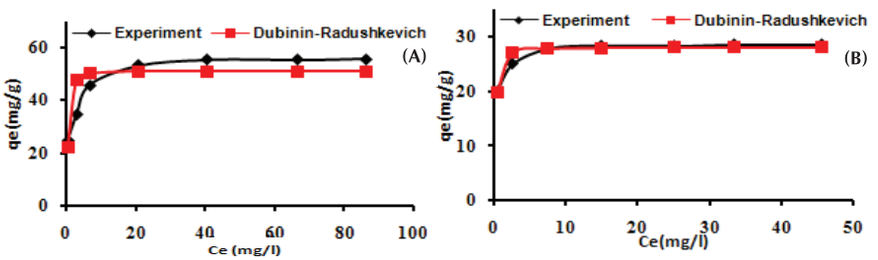

Fig. 8. Plots of non-linear isotherm Dubinin - Radushkevich models of γ-MnO_2 (A) and α-MnO_2 (B).

adsorption, this effect was not mentioned in the present study. Therefore, a range of pH values was chosen from 2.0 to 5.5. As a result, the maximum adsorption capacity obtained at pH=4.0 for both α- and γ-MnO_2 nano-adsorbents was approximately 94.96% removal for α-MnO_2 and nearly 98.90% removal for γ-MnO_2.

Figure 4B shows that the adsorption increases with the increase in the contact time and reaches equilibrium after 80 minutes for α-MnO_2 and 60 minutes for γ-MnO_2. However, the adsorption capacity of γ-MnO_2 was better than that of α-MnO_2 at any time.

Adsorption models studies

Isotherm models:

In order to predict adsorption mechanisms and assess the adsorption capacities of α- and γ-MnO_2 materials, four models namely Langmuir, Freundlich, Temkin, and Dubinin - Raduskevich were chosen and fitted with the experimental data.

On the one hand, Langmuir model assumes the uptake of Zinc(II) onto both materials to be monolayer adsorption. Plots of Langmuir models in Fig. 5 and non-linear isotherm Langmuir models parameters given in Table 4 provided that the experimental data of the adsorption of Zinc(II) ions on α-MnO_2 fitted to the Langmuir model better than that of γ-MnO_2, which corresponded with higher R^2 value and smaller RMSE and χ^2 values. In contrast, the maximum capacity of α-MnO_2 (28.50 mg/g) was two times less than that of γ-MnO_2 (55.23 mg/g). It was completely concordant with the porous structure of γ-MnO_2 with many adsorption sites.

On the other hand, Freundlich model assumes the adsorption of Zinc(II) ions as the multilayer adsorption and the interaction between adsorbate and absorbent. As shown in Fig. 6 and

Table 4. Isotherm equilibrium parameters.

Isotherm	Nonlinear forms	Isotherm Parameters		
			γ-MnO_2	α-MnO_2
Langmuir	$q_e = \frac{q_m.K_L.C_e}{1+K_L.C_e}$	K_L	0.0379	1.805
		q_m (mg/g)	55.23	28.76
		RMSE	0.619	0.1899
		R^2	0.9928	0.9877
		χ^2	0.0561	0.0078
Freundlich	$q_e = K_F.C_e^{1/n}$	n	3.17	18.79
		K_F	10.19	23.44
		RMSE	1.036	0.687
		R^2	0.9798	0.8395
		χ^2	0.2031	0.1089
Temkin	$q_e = \frac{RT}{b_T} Ln(K_T C_e)$	K_T (l/mg)	0.4156	$7.34.10^6$
		b_T(kJ/mol)	0.21	1.69
		RMSE	0.6380	0.6544
		R^2	0.9923	0.8542
		χ^2	0.0693	0.0981
Dubinin - Radushkevich	$q_e = q_m.e^{(-\beta.\varepsilon^2)}$	q_m (mg/g)	44.16	28.17
		β	57.13	0.2859
		E (kJ/mol)	0.094	1.32
		RMSE	2.262	0.2972
		R^2	0.9037	0.9699
		χ^2	0.8348	0.0192

Table 4, the experimental data of the uptake onto α-MnO_2 did not fit well to Freundlich model as γ-MnO_2 did. In addition, Zinc(II) ions could interact with γ-MnO_2 stronger than α-MnO_2 because of the smaller n value of γ-MnO_2. Nevertheless, the interactions between Zinc(II) and both materials were favourable since the 1/n values of α-MnO_2 (0.0505) and γ-MnO_2 (0.1425) were less than 1.

Temkin and Dubinin-Raduskevich models were used to estimate the heat of the adsorption and the mean free energy of the uptake of Zinc(II) ions onto both materials. Fig. 7, Fig. 8 and Table 4 showed that the experimental data fitted to Temkin model better than Dubinin-Radushkevich model for γ-MnO_2; whereas, α-MnO_2 followed Dubinin - Radushkevich model. Energy values calculated from both models to be less than 8 kJ/mol provided that there was a weak interaction between the absorbent and adsorbate [16] and the adsorption of Zinc(II) ions onto α-MnO_2 and γ-MnO_2 was essentially a physical process [8].

Kinetic models:

The uptake rate of Zn^{2+} ions onto α-MnO_2 and γ-MnO_2 surface was described by three kinetic models, namely pseudo-first-order, pseudo-second-order, and intra-particle diffusion model. The calculated results showed that although the adsorption process partially followed both pseudo-first-order and pseudo-second-order equations for different time, the adsorption of Zinc(II) ions onto both materials was controlled by the pseudo-second-order model because of its higher R^2 values (Fig. 9 and Table 2). In addition, intra-particle diffusion model developed by Weber and Morris [17] was applied to identify the diffusion mechanism involved in the adsorption process. Fig. 10 showed that there were three stages in the uptake of Zn^{2+} ions onto both α-MnO_2 and γ-MnO_2 surfaces. In the first one, Zn^{2+} ions were transferred from the solution to the material's surfaces. A gradual adsorption stage, in which the intra-particle diffusion was the controlling factor, was occurred in the second part. However, the plot did not pass through the origin. It was thereby concluded that the sorption can be controlled by two or more diffusion mechanisms [18]. The last one constituted the final equilibrium stage where the intra-particle diffusion started to decelerate. This can be explained that firstly, Zn^{2+} ion concentration in the solution was extremely low; and secondly, the adsorbent equilibrium was obtained when the number of adsorption sites decreased [19].

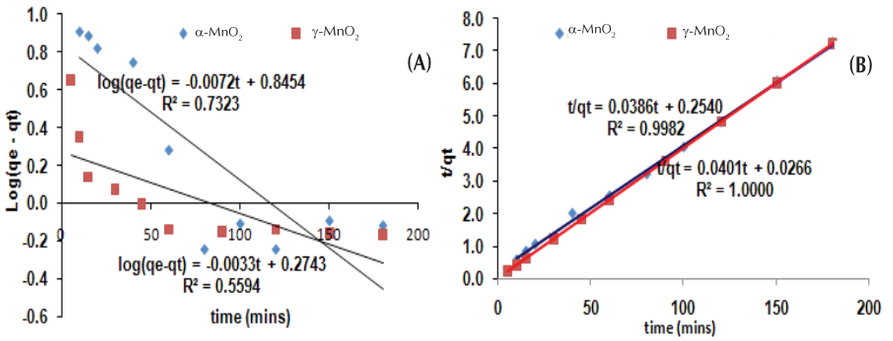

Fig. 9. Plots of pseudo-first-order (A), pseudo-second-order (B).

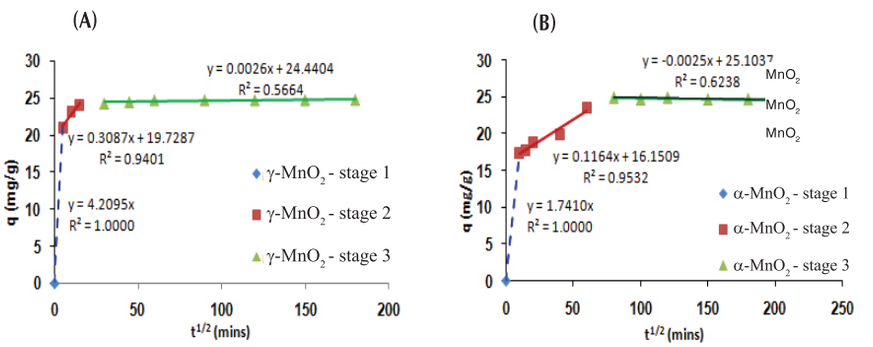

Fig. 10. Plots of intra-particle diffusion models of γ-MnO_2 (A) and α-MnO_2 (B).

Conclusions

To our knowledge, the comparison of the uptake of Zinc(II) ions onto α-MnO_2 and γ-MnO_2 nanomaterials in the optimal condition (4.0 of pH, 80 minutes of shaking time for α-MnO_2 and 60 minutes for γ-MnO_2, and 40-200 mg/l of initial concentration) is the first report. The results indicated that the maximum adsorption capacity calculated from Langmuir for γ-MnO_2 material was nearly two times higher than α-MnO_2. Energy values estimated from Temkin and Dubinin - Radushkevich models to be less than 8 kJ/mol informed that the uptake of Zinc(II) ions onto both materials was essentially a physical process. Kinetic studies showed that the adsorption data was well represented by pseudo-second-order models and the uptake of Zinc(II) ions onto both materials followed three stages.

REFERENCES

[1] H. Ullah, S. Noreen, Fozia, A. Rehman, A. Waseem, S. Zubair, M. Adnan, I. Ahmad (2017), "Comparative study of heavy metals content in cosmetic products of different countries marketed in Khyber Pakhtunkhwa, Pakistan", *Arabian Journal of Chemistry,* **10(1)**, pp.10-18.

[2] C. Gakwisiri, N. Raut, A. Al-Saadi, S. Al-Aisri, A. Al-Ajmi (2012), "A Critical Review of Removal of Zinc from Wastewater", In*: Proceedings of the World Congress on Engineering,* London, U.K., p.4.

[3] M.A. Barakat (2011), "New trends in removing heavy metals from industrial wastewater", *Arabian Journal of Chemistry*, **4(4)**, pp.361-377.

[4] K.S. Tushar, G. Dustin (2011), "Adsorption of zinc (Zn^{2+}) from aqueous solution on natural Bentonite", *Desalination and Water Treatment,* **267(2-3)**, pp.286-294.

[5] M. Minceva, L. Markovska, V. Meshko (2007), "Removal of Zn^{2+}, Cd^{2+} and Pb^{2+} from binary aqueous solution by natural zeolite and granulated activated carbon", *Macedonian Journal of Chemistry and Chemical Engineering*, **26(2)**, pp.125-134.

[6] K. Abidin, H. Ali (2005), "Oren adsorption of zinc from aqueous solutions to bentonite", *Journal of Hazardous Materials*, **125(1-3)**, pp.183-189.

[7] K. Rout, M. Mohapatra, B.K. Mohapatra, S. Anand (2009), "Pb(II), Cd(II) and Zn(II) adsorption on low grade manganese ore", *International Journal of Engineering, Science and Technology*, **1(1)**, pp.106-122.

[8] R.R. Bhatt, B.A. Shah (2015), "Sorption studies of heavy metal ions by salicylic acid-formaldehyde-catechol terpolymeric resin: Isotherm, kinetic and thermodynamics", *Arabian Journal of Chemistry*, **8(3)**, pp.414-426.

[9] C. Necla, R.K. Ali, A. Salih, G.S. Eda, A. Ihsan (2011), "Adsorption of Zinc(II) on diatomite and manganese-oxide-modified diatomite: A kinetic and equilibrium study", *Journal of Hazardous Materials*, **193**, pp.27-36.

[10] J. Li, B. Xi, Y. Zhu, Q. Li, Y. Yan, Y. Qian (2011), "A precursor route to synthesize mesoporous γ-MnO_2 microcrystals and their applications in lithium battery and water treatment", *J. Alloy. Compd.*, **509(39)**, pp.9542-9548.

[11] L. Ngoc Chung, D. Van Phuc (2015), "Sorption of lead(II), cobalt(II) and copper(II) ions from aqueous solutions by γ-MnO_2 nanostructure", *Adv. Nat. Sci.: Nanosci. Nanotechnol.*, **6(2)**, 025014.

[12] V.P. Dinh, N.C. Le, T.P.T. Nguyen, N.T. Nguyen (2016), "Synthesis of α-MnO_2 Nanomaterial from a Precursor γ-MnO_2: Characterization and Comparative Adsorption of Pb(II) and Fe(III)", *Journal of Chemistry*, **2016(2016)**, 8285717.

[13] K.Y. Foo, B.H. Hameed (2010), "Insights into the modeling of adsorption isotherm systems", *Chemical Engineering Journal*, **156(1)**, pp.2-10.

[14] C.P.J. Isaac, A. Sivakumar (2013), "Removal of lead and cadmium ions from water using Annona squamosa shell: kinetic and equilibrium studies", *Desalination and Water Treatment*, **51(40-42)**, pp.7700-7709.

[15] A. Heidari, H. Younesi, Z. Mehraban, H. Heikkinen (2013), "Selective adsorption of Pb(II), Cd(II), and Ni(II) ions from aqueous solution using chitosan-MAA nanoparticles", *Int. J. Biol. Macromol.*, **61**, pp.251-263.

[16] J. Anwar, U. Shafique, Waheed-uz-Zaman, M. Salman, A. Dar, S. Anwar (2010), "Removal of Pb(II) and Cd(II) from water by adsorption on peels of banana", *Bioresource Technology*, **101(6)**, pp.1752-1755.

[17] W.J. Weber, J.C. Morris (1963), "Kinetics of adsorption carbon from solutions", *Journal Sanitary Engeering Division: Proceedings of American Society of Civil Engineers*, **89(2)**, pp.31-60.

[18] S. Vasiliu, I. Bunia, S. Racovita, V. Neagu (2011), "Adsorption of cefotaxime sodium salt on polymer coated ion exchange resin microparticles: Kinetics, equilibrium and thermodynamic studies", *Carbohyd. Polym.*, **85(2)**, pp.376-387.

[19] F.C. Wu, R.L. Tseng, R.S. Juang (2000), "Comparative adsorption of metal and dye on flake- and bead-types of chitosans prepared from fishery wastes", *Journal of Hazardous Materials*, **73(1)**, pp.63-75.